

Cascade frequency generation regime in an optical parametric oscillator

D.B. Kolker, A.K. Dmitriev, P. Gorelik, F. Wong, J.-J. Zondy

Abstract. In a parametric oscillator of a special two-sectional design based on a lithium niobate periodic structure, a cascade frequency generation regime was observed in which a signal wave pumped a secondary parametric oscillator, producing secondary signal and idler waves. The secondary parametric oscillator can be tuned in a broad range of ~ 200 nm with respect to a fixed wavelength of the primary idler wave.

Keywords: parametric oscillator, cascade regime, frequency standard.

1. Introduction

At present the development of universal precision optical sources in the IR range attracts great interest. Optical parametric oscillators (OPOs) are used as radiation sources in optical spectrometers and for creation of new frequency standards. Self-phase-locked OPOs can be used in quantum-information problems for coding information in the intensity-phase coordinates [1]. A self-phase-locked OPO stabilised by saturated absorption resonances at vibrational–rotational transitions with small rotational numbers in methane can be used as a reference for a femtosecond optical synthesiser.

A cascade two-sectional OPO is a promising source of coherent optical radiation at five frequencies which can be specified by the choice of appropriate sections in the periodically polarised structure of lithium niobate. The five-frequency generation regime was demonstrated in a two-resonator OPO, which was initially used for frequency division by three [1–4]. In this paper, we fabricated a cascade OPO generating the primary and secondary signal

and idler waves. It was shown theoretically and confirmed experimentally that the five-frequency regime in the regime of frequency division by three is also degenerate.

2. A cascade OPO

A double-resonator OPO was pumped by a 5-W Verdi (Coherent) laser, the threshold power being $P_{th} = 25 - 35$ mW (Fig. 1). As a nonlinear element, a two-sectional periodically-poled lithium niobate crystal of size $10 \times 0.5 \times 20$ mm was used. The first section of length 13 mm with the structure period $\Lambda_{OPO} = 7.2$ μm was used for parametric generation, while the second structure, with a variable period $\Lambda_{SHG} = 19.45 - 19.75$ μm was used for the signal frequency doubling. The crystal was thermally stabilised at 205 °C. To observe clusters* at $\lambda_s \sim 800$ nm (signal wave) and $\lambda_i \sim 1600$ nm (idler wave), the asymmetric resonator of the OPO (with the intermode interval 1500 MHz) was scanned by applying a saw-tooth voltage across a piezoelectric ceramics on which one of the resonator mirrors was mounted.

Figure 2 presents cluster structures for pump waves and signal and idler waves for the pump power not exceeding the lasing threshold of the secondary OPO. A saw-tooth voltage from the generator was applied to the piezoelectric ceramics with one of the OPO resonator mirrors mounted on it. In this case, the behaviour of clusters remained conventional [1, 2]. As the threshold pump power e_{p1} was achieved, the pump depletion was observed when the energy from the pump wave was transferred to the signal and idler waves.

As the pump power was increased, the radiation power at the signal wave frequency was saturated and increased at the idler wave frequency. When the OPO pump power was increased above 70 mW (the secondary generation threshold), the stable saturation of the radiation power was observed at the signal wave frequency, and the signal at the idler wave frequency further increased (Fig. 3). In this case, the signal wave is in fact a pump source for the secondary OPO, which is formed by the second section of the nonlinear lithium niobate crystal, and produces the secondary signal and idler waves. In this situation, the five-frequency generation is achieved in the OPO at frequencies of the pump and primary and secondary signal and idler waves. Figure 4 presents the OPO emission spectrum in the 1596-nm region recorded with an optical spectrum analyser.

J.-J. Zondy Institute National de Metrology, Conservatoire National des Arts et Metres, 61 rue du Landy, 93210, La Plaine St. Denis, France;
D.B. Kolker, A.K. Dmitriev Novosibirsk State Technical University, Karl Marx prosp. 20; Institute of Laser Physics, Siberian Branch, Russian Academy of Sciences, prosp. Lavrent'eva 13/3, 630090 Novosibirsk, Russia; e-mail: dkolker@mail.ru, dak@ftf.nstu.ru;
P. Gorelik, F. Wong Massachusetts Institute of Technology, Cambridge, MA 02139, USA

Received 3 April 2008; revision received 9 September 2008
 Kvantovaya Elektronika 39(5) 431–434 (2009)
 Translated by M.N. Sapozhnikov

*A cluster is a set of OPO modes combined in groups and appearing during the OPO scan [1].

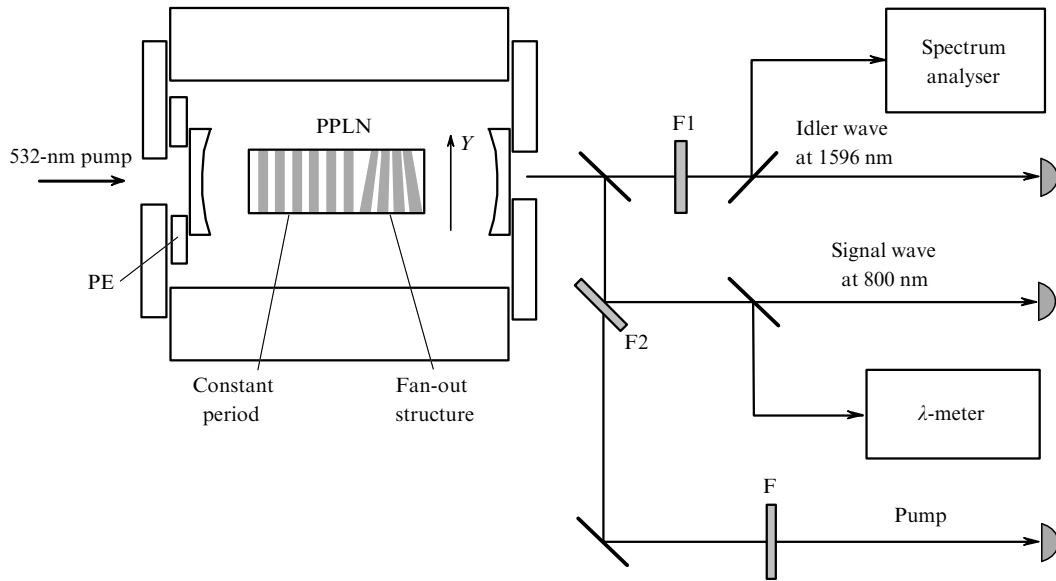


Figure 1. Scheme of the experimental setup: (F1) filter transmitting the idler wave; (F2) filter transmitting pump radiation and reflecting the signal wave; (PPLN) periodically-poled lithium niobate domain structure; (PE) piezoelectric element; (F) filter transmitting pump radiation.

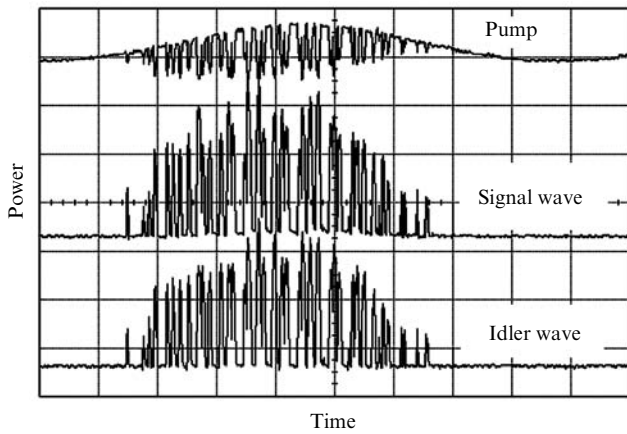


Figure 2. Shape of clusters during the scan of a resonator in a conventional OPO.

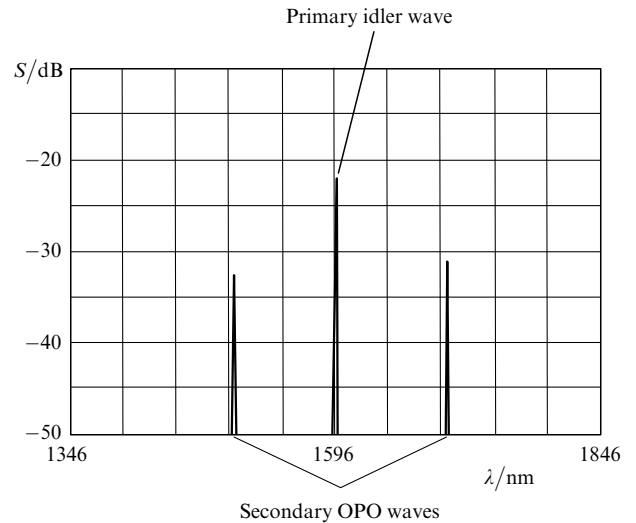


Figure 4. Spectral power of the S-cascade OPO in the 1596-nm region.

Figure 5 demonstrates the tuning range of the secondary OPO with respect to the fixed frequency of the primary OPO. The secondary OPO was tuned by moving the lithium

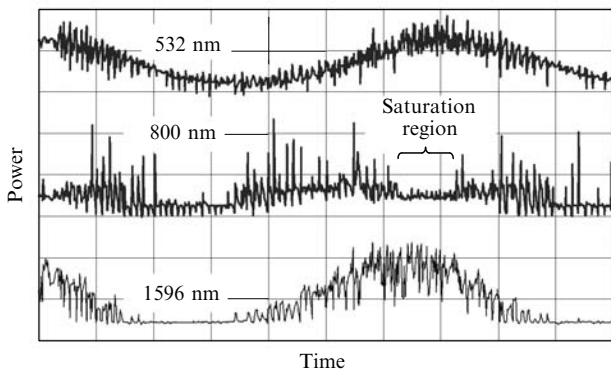


Figure 3. Stable saturation of the signal wave power with increasing pump power (321 mW) and using a two-sectional PPLN.

niobate crystal along the Y axis (Fig. 1). In this case, the primary-signal-wave frequency did not change because the structure period in the first OPO section remained invariable, while this period in the second section was varied within 200 nm due to the displacement of the crystal along the Y axis.

When the OPO pump power was changed from 60 to 300 mW, the output power of the secondary OPO in the 1596-nm region changed from 0.5 to 15 mW, the output power at the primary-signal-wave frequency varying from 5.8 to 6.2 mW and saturating at the OPO pump power corresponding to the generation threshold of the secondary OPO (Fig. 6).

3. Theoretical model of a cascade OPO

We represent the time derivatives of the complex amplitudes of fields for a nondegenerate OPO in the case of exact

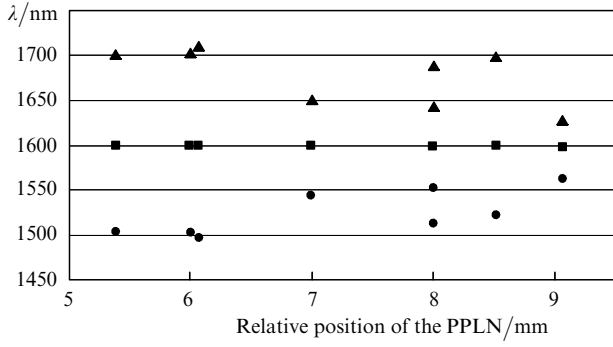


Figure 5. Tuning ranges of the secondary OPO upon the change in the PPLN position along the Y axis for the secondary idler (▲), primary idler (■) and secondary signal (●) waves.

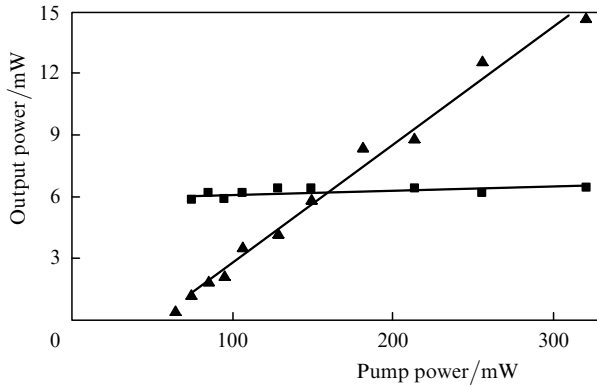


Figure 6. Dependences of the output power of the cascade OPO at the primary- (■) and secondary- (▲) signal-wave frequencies on the pump power at 532 nm.

coincidence of its resonator frequencies with idler- and signal-wave frequencies in the form

$$\dot{A}_p = -\kappa_p A_p - \chi_1 A_s A_i + \sqrt{2\kappa_p} e_p, \quad (1)$$

$$\dot{A}_s = -\kappa_s A_s - \chi_1 A_p A_i^* - \chi_2 A_+ A_-, \quad (2)$$

$$\dot{A}_i = -\kappa_i A_i - \chi_1 A_p A_s^*, \quad (3)$$

$$\dot{A}_+ = -\kappa_+ A_+ - \chi_2 A_s A_-^*, \quad (4)$$

$$\dot{A}_- = -\kappa_- A_- - \chi_2 A_s A_+^*. \quad (5)$$

Here, $A_{p,s,i}$ are complex field amplitudes at the pump-, signal- and idler-wave frequencies; $\kappa_{p,s,i}$ are losses per round trip in the resonator at the pump-, signal-, and idler-wave frequencies of the primary OPO; κ_+ and κ_- are similar losses at the signal- and idler-wave frequencies of the secondary OPO; χ_1 and χ_2 are second-order nonlinearities for the first and second sections in the nonlinear lithium niobate element; and e_p is the input pump power (in photon s^{-1}).

Let us represent the complex amplitude in the form $A_j = r_j \exp(i\phi_j)$, where $j = p, s, i$. Under the condition $\dot{A}_j = 0$, we obtain the stationary solutions of system (1)–(5) for two regimes: above the threshold for the primary OPO, but below the threshold for the secondary OPO, and above the thresholds of both the primary and secondary OPOs. Let us assume that $\chi_2 = 0$ and write stationary

solutions only for the primary OPO in the case of the zero detuning of the resonator. It is obvious that the intracavity pump field saturates. Then, we have

$$\phi_p = \phi_s + \phi_i, \quad r_p^2 = \kappa_s \kappa_i / \chi_1^2, \quad (6)$$

$$2\kappa_s r_s^2 = 2\kappa_i r_i^2 = 4e_{p1}^2 (e_p / \tilde{e}_p - 1), \quad (7)$$

$$e_{p1}^2 = \kappa_p \kappa_s \kappa_i / (2\chi_1^2). \quad (8)$$

In these equations, $r_{p,s,i}$ are the intracavity fields of the pump, signal, and idler waves; $\phi_{p,s,i}$ are phases of the corresponding waves; and e_{p1} and \tilde{e}_p are the threshold pump powers for the primary and secondary OPOs.

Note that the conversion efficiency in expression (7) is proportional to the square root of the pump power e_p . At high pump powers, the signal wave field achieves the value sufficient for ‘switching on’ the secondary OPO at nonzero amplitudes A_+ and A_- . Let us write stationary solutions for a complete system of equations

$$\phi_p = \phi_s + \phi_i, \quad \phi_s = \phi_+ + \phi_-, \quad (9)$$

$$2\kappa_s r_s^2 = 2\kappa_+ \kappa_- / \chi_2^2 \equiv 4e_{p2}^2, \quad (10)$$

$$2\kappa_+ r_+^2 = 2\kappa_- r_-^2 = 4e_{p2}^2 (e_p^2 / \tilde{e}_p^2 - 1), \quad (11)$$

$$2\kappa_p r_p^2 = 4e_{p1}^2 e_p^2 / \tilde{e}_p^2, \quad 2\kappa_i r_i^2 = 4e_{p2}^2 e_p^2 / \tilde{e}_p^2, \quad (12)$$

$$\tilde{e}_p^2 = e_{p2}^2 (1 + e_p^2 / e_{p1}^2)^2, \quad (13)$$

where ϕ_+ and ϕ_- are the phases of the signal and idler waves of the secondary OPO; r_+ and r_- are the intracavity fields of these waves; and e_{p2} is the pump power of the primary OPO at the output of the periodic domain structure.

If the pump radiation is not resonant with the OPO resonator and κ_p greatly exceeds other intracavity losses ($e_{p1} \gg e_{p2}$), the threshold power e_p of the secondary OPO will slightly exceed the threshold power \tilde{e}_p of the primary OPO. In the presence of the secondary OPO, the external pump field r_p is not saturated. In this case, as follows from (10), the intracavity field r_s of the primary signal wave saturates, and the optical limitation of the amplitude A_s occurs in the cascade OPO. Note that in the degenerate case ($A_+ = A_- = A_i$) the self-phase locking is observed [5], and the static behaviour of the system considerably differs from dynamic behaviour. In this case, neither the pump nor signal wave is saturated, and the output power at the signal- and idler-wave frequencies is lower than that for a conventional single-sectional OPO.

Indeed, compared to a conventional OPO, the cascade OPO is a more efficient source of coherent radiation converting the pump power to the power of secondary signal and idler waves, which linearly depends on the pump power.

4. Conclusions

The cascade regime of parametric generation opens up the possibilities for creation of cw five-frequency OPOs with specified frequency combinations, which are determined by periods A_{OPO} and A_{SHG} of the corresponding section of a

periodically polarised lithium niobate or KTP structure. A special fan-out design of the nonlinear element structure allows tuning the secondary OPO in a broad range of ~ 200 nm irrespective of the primary OPO. In this case, the frequencies of the primary OPO do not change because the structure period in the first section of the OPO is independent of the transverse coordinate.

The tunable cascade OPO allows one to control phase matching for the secondary OPO independently of the primary OPO. The output power of the secondary OPO linearly depends on the OPO pump power. We obtained tuning in a broad range of ~ 200 nm. The self-phase locking for the signal and idler waves was observed in the two-resonator OPO when the pump-, signal-, and idler-wave frequencies were in the relation 3 : 2 : 1 [3–6]. In this case, the five-frequency regime was also degenerate.

The system developed in the work can be used as a source of coherent radiation tunable in the entire transparency range of lithium niobate for spectroscopic, metrological and other applications.

Acknowledgements. This work was supported by programs DoD MURI (Grant No. N00014-02-1-0717) and MIT-France Seed Fund.

References

1. Zondy J.-J. et al. *Phys. Rev. A*, **63**, 023814 (2001).
2. Zondy J.-J. *Phys. Rev. A*, **67**, 03581 (2003).
3. Zondy J.-J., Kolker D., Wong F.N.C. *Phys. Rev. Lett.*, **93**, 043902 (2004).
4. Kolker D., Dmitriyev A., Gorelik P.V., Wong F.N.C., Zondy J.-J. *Laser Phys.*, **18** (6), 794 (2008).
5. Gorelik P.V., Wong F.N.C., Kolker D., Dmitriyev A., Zondy J.-J. *Proc. ICONO 2007* (Minsk, Belarus, 2007).
6. Zondy J.-J., Kolker D., Wong F.N.C. *Proc. MPLP 2004* (Novosibirsk, Russia, 2004).